

letters

Prediction and confirmation of a site critical for effector regulation of RGS domain activity

Mathew E. Sowa^{1,2,6}, Wei He¹, Kevin C. Slep⁸, Michele A. Kercher^{7,8}, Olivier Lichtarge^{2,3,4,5} and Theodore G. Wensel^{1,2,6}

¹Verna and Marrs McLean Department of Biochemistry and Molecular Biology, ²Program in Structural and Computational Biology and Molecular Biophysics, ³Department of Molecular and Human Genetics, ⁴Program in Developmental Biology, ⁵Human Genome Sequencing Center, Baylor College of Medicine, Houston, Texas 77030, USA. ⁶W.M. Keck Center for Computational Biology, Houston, Texas 77030, USA. ⁷Howard Hughes Medical Institute, ⁸Department of Molecular Biophysics and Biochemistry, Yale University, New Haven, Connecticut 06511, USA.

A critical challenge of structural genomics is to extract functional information from protein structures. We present an example of how this may be accomplished using the Evolutionary Trace (ET) method in the context of the regulators of G protein signaling (RGS) family. We have previously applied ET to the RGS family and identified a novel, evolutionarily privileged site on the RGS domain as important for regulating RGS activity. Here we confirm through targeted mutagenesis of RGS7 that these ET-identified residues are critical for RGS domain regulation and are likely to function as global determinants of RGS function. We also discuss how the recent structure of the complex of RGS9, $G_{\alpha_{i1\alpha}}$ -GDP-AIF₄⁻ and the effector subunit PDE γ confirms their contact with the effector-G protein interface, forming a structural pathway that communicates from the effector-contacting surface of the G protein and RGS catalytic core domain to the catalytic interface between G_{α} and RGS. These results demonstrate the effectiveness of ET for identifying binding sites and efficiently focusing mutational studies on their key residues, thereby linking raw sequence and structure data to functional information.

It is known that multiple RGS proteins, or their catalytic cores, are able to activate a given species of G_{α} *in vitro*; conversely, individual RGS proteins can accelerate the GTPase rates of a variety of G_{α} subunits¹. In light of this promiscuity of RGS proteins and of the need for G_{α} inactivation through GTP hydrolysis to be precisely

	a	b	c	d	e	f
RGS9:	S F ³¹⁴ H F ³¹⁴ ... K ³¹⁴ F L A P G A ³⁶⁰ R ³⁶⁰ W ³⁶² I N I D ³⁶⁷ G ³⁶⁷ K T M ³⁷⁰ D					
RGS7:	Q F ³⁴⁸ K F ³⁴⁸ ... Q ³⁴⁸ F L A P G A ³⁸⁷ S ³⁸⁷ A I N L D ⁴⁰¹ S ⁴⁰¹ K S Y ⁴⁰⁴ D					
RGS4:	A F ¹¹⁰ K ¹¹⁰ A F ¹¹⁰ ... N ¹¹⁰ F I S V Q A ¹²⁴ K ¹²⁴ V N L D ¹³¹ S ¹³¹ C T E ¹³⁴					
RGS16:	A F ¹⁵⁷ H ¹⁵⁷ A F ¹⁵⁷ ... E ¹⁵⁷ F I C S E A ¹⁵⁹ K ¹⁵⁹ V N I D ¹⁶⁴ H ¹⁶⁴ E T R ¹⁶⁷ E ¹⁷⁰					

Fig. 1 Sequence alignment of selected RGS domains. Selected portions of bovine RGS9, mouse RGS7, rat RGS4 and human RGS16 are aligned for easy comparison of residue numbers. Red = Trace residues, dark red boxes = Trace residues mutated in RGS7 mutant constructs to those in RGS9. Lower case letters are used for generic identification of corresponding sequence positions in different RGS proteins.

tuned to changing cellular conditions, an outstanding problem for understanding RGS function is to determine how regulation and discrimination are achieved by interactions with other protein domains²⁻⁸ and lipids⁹⁻¹³. We have previously applied the Evolutionary Trace (ET) method¹⁴ to the RGS family in order to identify residues in the RGS domain that provide sites for regulation of RGS activity¹⁵, with a focus on the mammalian RGS protein, RGS9-1, whose physiological function and regulation are best understood through biochemical^{16,17} and gene-inactivation¹⁸ studies. RGS9-1 is the GTPase accelerating protein (GAP) for vision¹⁶ and acts to provide fine-tuning of the cascade through regulating $G_{\alpha_{i1}}$ transducin, the G protein of phototransduction. *In vitro*, the RGS9-1 RGS domain can accelerate the rate of $G_{\alpha_{i1}}$ GTP hydrolysis; however, this rate is still not enough to account for the ~200 ms recovery of rod cells. Only when the γ subunit of $G_{\alpha_{i1}}$'s effector, cGMP phosphodiesterase (PDE), is added to RGS9-1/ $G_{\alpha_{i1}}$ does the GTPase rate approach that required for *in vivo* recovery¹⁹.

ET analysis combines sequence and structure data to infer the location of functional sites in proteins. This is done by dividing the members of a protein family into functional classes based on its sequence identity tree, identifying the residues that are invariant within every class yet vary among them, and mapping these so-called class specific, or Trace residues onto a representative structure. Since each class corresponds to a different variation of the common function of the family, variations in class specific residues are always associated with changes in this function. The clustering of these class specific residues on the protein structure indicates an evolutionarily privileged site that is likely to impart the functional specificity of individual family members¹⁴. Initial validations have been consistent with experimental data²⁰⁻²², but

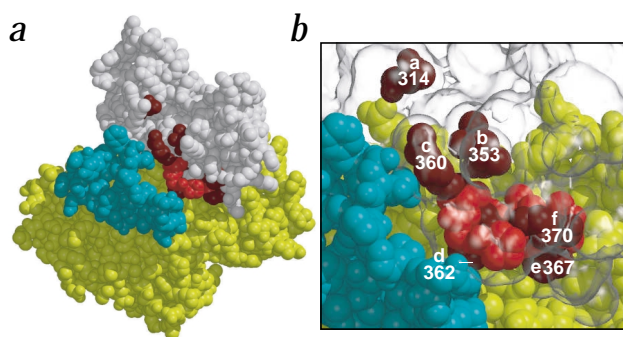


Fig. 2 An effector-proximal surface on RGS9 defined by Trace residues. **a**, The structure of the complex of the RGS9 domain, $G_{\alpha_{i1\alpha}}$ chimera and the C-terminal 38 amino acids of PDE γ confirms our ET based prediction of the RGS-PDE γ binding site. Trace residues displayed on the structure are those previously hypothesized to form the effector-GAP interface (314, 353, 357-360, 362-364)¹⁵ and G_{α} contact residues 367 and 370 (since these two residues were selected for mutation). PDE γ residue Val 66 is in contact with RGS9 Trace residue Trp 362, and PDE γ Asp 52 is in close proximity to RGS9 Arg 360. The remaining Trace residues form a swath that parallels the PDE γ interaction surface on $G_{\alpha_{i1\alpha}}$. **b**, Expanded view of (a) to illustrate more clearly residues that were mutated. In (a), white = RGS9; in (b), clear = RGS9 solvent accessible surface (generated by GRASP²⁶); in (a,b), yellow = $G_{\alpha_{i1\alpha}}$, cyan = PDE γ , red = Trace residues, dark red = residues with non-conservative substitutions between RGS9 and RGS7 selected for mutation in RGS7. Letters correspond to general residue positions (see Fig. 1). Molecular graphics were produced using Molscript²⁷ and Raster3D²⁸.

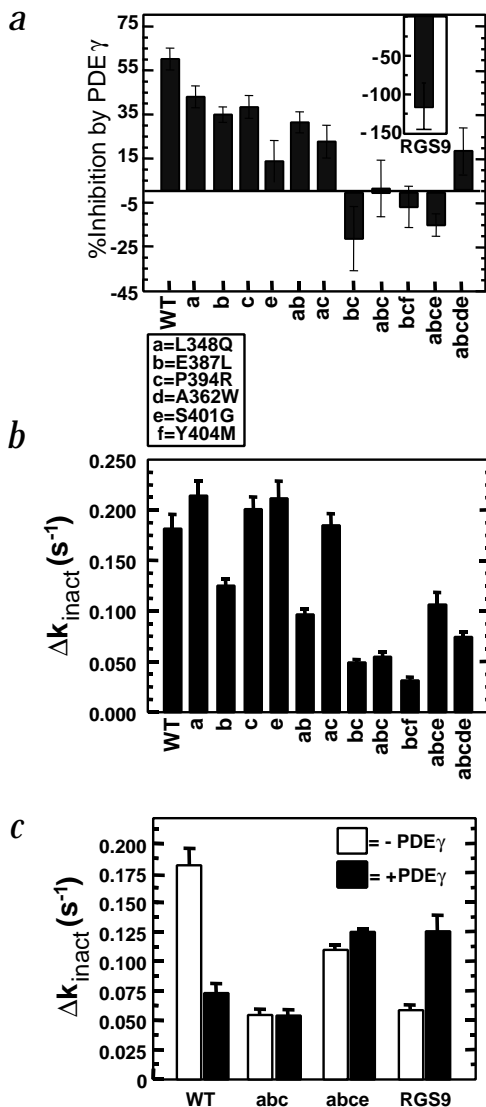


Fig. 3 Results of ET based targeted mutagenesis of the RGS7 domain. **a**, This plot shows the percent by which each protein was inhibited in the presence of PDE γ ; $[1 - (\Delta k_{\text{inact}}(+\text{PDE}\gamma) / \Delta k_{\text{inact}}(-\text{PDE}\gamma))] \times 100\%$. Negative numbers represent enhancement. The inset shows the enhancement of the catalytic core of RGS9 by PDE γ . **b**, Plot of the basal GAP activity of each mutant (see Methods). **c**, Construct *abc* has a Δk_{inact} similar to PDE γ inhibited WT RGS7 and there is no effect in the presence of PDE γ . When residue Ser 401 (e), located at the RGS-G α interface, is substituted as well, the resulting protein (abce) has a Δk_{inact} approximately the same as PDE γ enhanced RGS9, and shows little change in activity upon the addition of PDE γ .

ties were not the same in RGS9 and any RGS protein known to be inhibited by PDE γ . Only six residues met these criteria (boxed residues in Fig. 1, designated a–f), and they were replaced alone or in combination with the corresponding residues in RGS9. We then measured the GAP activities of the resulting proteins in the presence and absence of PDE γ . Later, after the structure of the RGS9-G α -GDP-AIF $_4^-$ -PDE γ complex was determined²³, we examined the proximity of these residues to the G α -effector interface (Fig. 2).

The results obtained for the mutant proteins show a critical role for residues b and c (Fig. 3 and Table 1). The single mutations L348Q (a), E387L (b), and P394R (c) resulted in proteins that were still inhibited upon the addition of PDE γ (a = 42.5 ± 4.9%; b = 34.4 ± 3.5%; c = 37.8 ± 5.1%; Fig. 3a). Both a and c had basal GAP activities — that is, in the absence of PDE γ — similar to that of wild type (WT) RGS7 (a = 0.214 ± 0.015 s $^{-1}$, c = 0.201 ± 0.012 s $^{-1}$, WT RGS7 = 0.181 ± 0.014 s $^{-1}$; all rates are Δk_{inact} ; see Methods; Fig. 3b), whereas basal GAP activity of b was reduced by 30% (0.125 ± 0.006 s $^{-1}$; Fig. 3b). The double mutations L348Q/E387L (ab) and L348Q/P394R (ac) produced RGS7 mutant proteins that remained inhibited by PDE γ (30.9 ± 4.7% and 22.2 ± 7.5%, respectively; Fig. 3a), with the basal GAP activity of ab reduced by 50% (ab = 0.097 ± 0.005 s $^{-1}$) and ac approximately the same as WT RGS7 (ac = 0.185 ± 0.011 s $^{-1}$; Fig. 3b). The RGS7 double mutant E387L/P394R (bc) and triple mutant L348Q/E387L/P394R (abc) were not inhibited by PDE γ (Fig. 3a) and their basal GAP activities were slightly lower than that of the PDE γ -inhibited WT RGS7 (Fig. 3b), indicating that positions b and c are important for regulation of RGS domain activity.

In addition to positions b and c, site e also plays an important role for regulating the activity of the RGS domain. The S401G (e) mutation had little effect on basal GAP activity, yet significantly

until now no set of studies has tested whether ET predictions could anticipate functional information from both mutational and structure determination experiments.

ET analysis of the RGS family indicated that positions in RGS4 corresponding to RGS9 residues 314, 353, 357, 358, 360, 362, 367 and 370 (see Fig. 1 for sequence comparison) formed an evolutionarily privileged surface with no known function. Based on the pattern of amino acid identity of these residues in RGS proteins either inhibited (RGS7, 6, 16, 4 and GAIP) or enhanced (RGS9) by PDE γ , we hypothesized that this site would be involved in the PDE γ -mediated regulation of RGS GAP activity. We tested this hypothesis by generating site-specific mutations in the RGS domain of RGS7. Of all RGS proteins whose GAP activity is inhibited rather than enhanced by PDE γ , RGS7 is the one whose sequence is most similar to that of RGS9 (48% identity). In order to avoid testing all 65 non-identical residues in the RGS domain of RGS7 to determine which ones account for the functional differences between RGS7 and RGS9, we restricted our mutagenesis to all positions in the catalytic core of RGS7 that met two criteria: they were identified by ET to be part of a functionally important cluster of surface residues previously identified as ‘site 2’ (ref. 15; to distinguish them from ‘site 1’ residues already known to form the RGS-G α interface), and their identi-

Table 1 Summary of RGS7 mutagenesis¹

Protein	Δk_{inact} (s $^{-1}$) (- PDE γ)	Δk_{inact} (s $^{-1}$) (+ PDE γ)	% Inhibition by PDE γ
WT RGS7	0.181 ± 0.014	0.073 ± 0.007	59.6 ± 5.0
a	0.214 ± 0.015	0.123 ± 0.006	42.5 ± 4.9
b	0.125 ± 0.006	0.082 ± 0.002	34.4 ± 3.5
c	0.201 ± 0.012	0.125 ± 0.007	37.8 ± 5.1
e	0.212 ± 0.017	0.184 ± 0.014	13.2 ± 9.6
ab	0.097 ± 0.005	0.067 ± 0.003	30.9 ± 4.7
ac	0.185 ± 0.011	0.144 ± 0.011	22.2 ± 7.5
bc	0.048 ± 0.003	0.058 ± 0.006	-20.8 ± 14.6
abc	0.054 ± 0.005	0.053 ± 0.005	1.8 ± 13.0
bcf	0.031 ± 0.002	0.033 ± 0.002	-6.5 ± 9.4
abce	0.109 ± 0.004	0.125 ± 0.003	-14.7 ± 5.0
abcde	0.074 ± 0.006	0.061 ± 0.006	-17.6 ± 10.5
WT RGS9	0.058 ± 0.005	0.125 ± 0.014	-115.5 ± 30.5

¹ Δk_{inact} was calculated as described in the methods and the percent inhibition by PDE γ was calculated as $[1 - (\Delta k_{\text{inact}}(+\text{PDE}\gamma) / \Delta k_{\text{inact}}(-\text{PDE}\gamma))] \times 100\%$. Negative numbers represent enhancement by PDE γ . (a = L348Q, b = E387L, c = P394R, d = A362W, e = S401G, f = Y404M).

letters

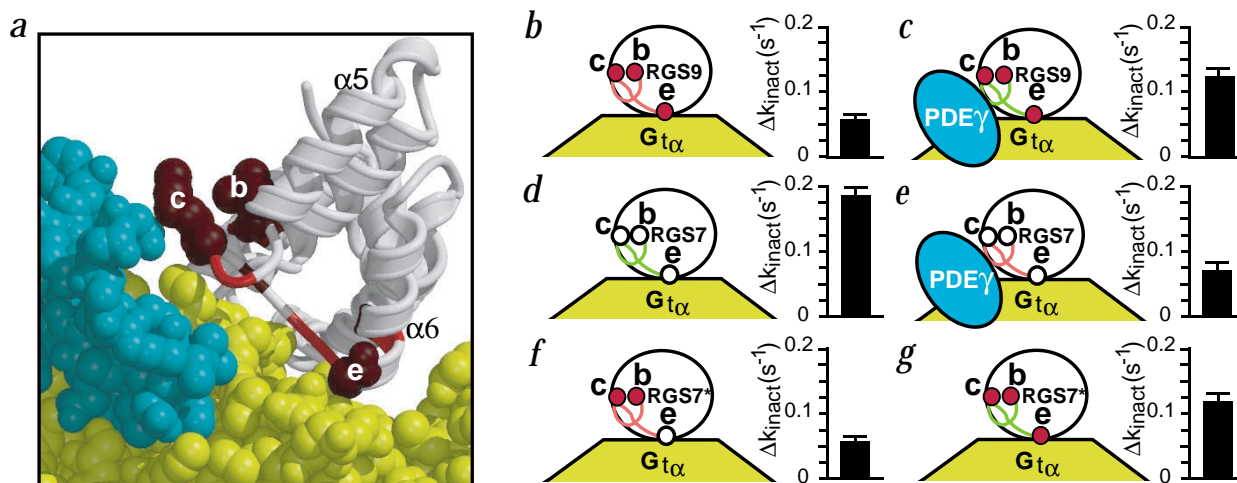


Fig. 4 A model for regulation of RGS activity *via* positions bc and e. **a**, Trace residues form a pathway including the $\alpha 5/\alpha 6$ connecting loop, position b, located N-terminal to the $\alpha 5/\alpha 6$ loop, and position e, located C-terminal to the loop, which may allow changes at bc to influence RGS catalytic activity at the G_{α} binding interface. The Gly at e in RGS9 allows greater backbone freedom than the Ser in RGS7, allowing for greater influence of PDE γ on the $\alpha 5/\alpha 6$ loop. The color scheme is the same as in Fig. 2. **b–g**, Trace residues at positions b and c are located in a position where they could influence the conformation of the $\alpha 5/\alpha 6$ connecting loop (shown as the line connecting b to e; low GAP activity = red line; high GAP activity = green line; RGS9 residues = dark red circles; RGS7 residues = white circles; RGS7* = mutant RGS7), and thus modulate the activity of the RGS domain (graphs to the right of the drawings). **b**, In the absence of G_{α} bound effector, the GAP activity of the RGS9 catalytic core domain is low. **c**, When G_{α} is bound to PDE γ , the activity of RGS9 is enhanced. **d**, RGS7 has a high activity when G_{α} is not bound to PDE γ . **e**, When PDE γ is bound to G_{α} , the activity of RGS7 is inhibited. **f**, Changes at positions b and c in RGS7 to their corresponding residues from RGS9 result in a protein that is similar to PDE γ -inhibited RGS7. **g**, When the RGS7 residue at position e is switched to its corresponding RGS9 residue in conjunction with the bc change, the resulting protein behaves similar to RGS9 bound to the G_{α} -PDE γ complex (Figs. 3c, 4c).

decreased the inhibitory effect of PDE γ (Fig. 3). The quadruple mutant L348Q/E387L/P394R/S401G (abce) actually displayed a slight stimulation by PDE γ ($14.7 \pm 5.0\%$; Fig. 3a) and it also had higher basal GAP activity than the abc mutant. Its GAP activity upon PDE γ addition was nearly identical to that of RGS9 with PDE γ ($0.125 \pm .002 \text{ s}^{-1}$ for abce + PDE γ versus $0.125 \pm 0.013 \text{ s}^{-1}$ for RGS9 + PDE γ ; Fig. 3c).

Sites d and f were tested in combination with mutations that displayed functional differences from wild type RGS7 and did not significantly alter their activity. The triple mutant E387L/P394R/Y404M (bcf) resembled the bc construct in its failure to be enhanced by PDE γ (Fig. 3a), but had reduced basal GAP activity ($bcf = 0.031 \pm 0.002 \text{ s}^{-1}$; Fig. 3b) compared to the bc construct ($bc = 0.048 \pm 0.003 \text{ s}^{-1}$). Adding the additional substitution of A396W (d) to produce the quintuple mutant L348Q/E387L/P394R/A396W/S401G (abcde) reverted the PDE γ enhancement in abce to inhibition (Fig. 3a), possibly due to restrictions imposed by having a Ser between c and d instead of an Arg. The behavior of abcde indicates that position d is not critical for the observed differences between RGS7 and RGS9, even though it is the residue most directly in contact with PDE γ ²³, while those at b and c (Glu 387 and Pro 394 in RGS7) clearly are, with some assistance from position e (Ser 401 in RGS7).

Our ET based mutational analysis of the RGS7 core domain shows that three residues selected for mutation have dramatic effects on the activity of RGS7 in both the presence and absence of PDE γ (b, c and e), while the other three had only slight effects (a, d and f). Keeping in mind that residues may be evolutionarily important for multiple functional or structural reasons, one explanation for this is that a, d, and f, are important for the regulation of RGS domains by factors other than PDE γ . Because residues identified by ET are functionally important for all members of the protein family, the regulatory role of positions b and c is expected to be common for other members of the RGS family,

acting as a global regulator of RGS activity in either the presence or absence of effectors or other regulatory components. The global importance of position e within the family is already confirmed by its role in direct interactions with G_{α} ^{23,24}.

After the ET-based mutational analysis of the RGS7 core domain was completed, the structure of the heterotrimeric complex of the RGS9 catalytic core domain, $G_{\alpha/11\alpha}$ -GDP- AlF_4^- , and PDE γ was solved by Slep *et al.*²³. This structure reveals that RGS9 residues from site 2 form the effector interaction site on the RGS domain, confirming our computational prediction (Fig. 2) and supporting our mutational analysis of RGS7. Specifically, our mutagenesis pinpoints positions b, c, and e as important for distinguishing the effector responses of RGS7 and RGS9. Not surprisingly, the structure of the effector-RGS- G_{α} complex shows that position b (Leu 353 in RGS9) orients c (Arg 360 in RGS9) which is in close proximity to the effector, while position e (Gly 367 in RGS9) directly contacts switch residues in G_{α} (Fig. 2).

What is made clear by the millions of years of evolutionary mutagenesis and selection assays embodied in ET analysis, is the role of the additional Trace residues in the $\alpha 5/\alpha 6$ loop. First, of the eleven residues 355–366 in this loop region, all but four (355, 356, 361 and 363) are Trace residues, indicating that this region is important for the functional specificity of the RGS family. This is consistent with the large conformational changes of the loop when RGS9 binds $G_{\alpha/11\alpha}$ ²³, suggesting that its orientation and composition play a major role in defining the activity of the RGS domains. Second, the mechanism by which sites b and c regulate catalytic activity must be an allosteric one because unlike site e, they are removed from the catalytic interface and must communicate with it, from a distance, through intervening residues, especially those in the vicinity of the $\alpha 5/\alpha 6$ connecting loop (Fig. 4a). Simultaneous substitution at positions b and c without a change at e gives rise to a constitutively inhibited protein — one whose basal GAP activity resembles that of PDE γ -inhibited RGS7 and which is therefore insensitive to inhibition by PDE γ



(Fig. 4e,f). In contrast, although adding a mutation at a to make abc has little effect, coupling abc substitutions with one at the G_{α} -contacting position e to produce abce yields a protein whose functional state more closely resembles that of PDE γ -stimulated RGS9 than that of RGS7 (Fig. 4c,g).

As the collection of sequences on a genomic scale continues to expand along with the somewhat slower but accelerating accumulation of structures, our ability to translate these vast amounts of data into functional information at the molecular level must increasingly rely on computational approaches. Our results show that the Evolutionary Trace can make predictions that anticipate both mutational and crystallographic studies, that are helpful for directing targeted mutagenesis experiments and that can act as a framework for interpreting their outcomes in the broad context of an entire protein family. This is an example of a new paradigm, whereby a computational approach utilizes the combination of structural data with the large record of evolutionary experiments implicit in DNA and protein sequences to accelerate the solution of daunting problems of protein structure and function.

Methods

Mutagenesis of the RGS7 catalytic core domain. The RGS7 catalytic core domain was cloned into the pGEX-2TK vector using added *Bam*HI and *Nde*I sites. Mutagenesis was performed on this construct (pGEX-RGS7d) using the Stratagene QuikChange™ site-directed mutagenesis kit with primers containing each point mutation. Mutations were confirmed by DNA sequencing.

Expression, purification, and activity of mutant RGS7 proteins. Mutant RGS7 constructs were transformed into *E. coli* BL21-DE3 (pLysS) cells for expression. Cells were grown at 30 °C for constructs a, b, e, ab, abce and abcde, and at 16 °C for the remaining constructs until the OD₆₀₀ was 0.6–0.8. Protein expression was induced by the addition of IPTG at a final concentration of 0.1 mM and cells were grown for 2–4 h (30 °C) or 20–24 h (16 °C) before harvesting and storage of cell pellets at -80 °C. Cells were lysed *via* sonication in SB (10 mM Tris, pH 7.6, 300 mM NaCl, 1% Triton X-100, 1 mM DTT) and cleared lysate was incubated with GSH-Sepharose with gentle shaking for 2 h at 4 °C. This mixture was added to a column and washed with SB (without Triton X-100) until no further protein was found in the flow through, and then SB was exchanged for GAPN buffer (10 mM Tris, pH 7.4, 100 mM NaCl, 2 mM MgCl₂, 1 mM DTT). Protein was eluted in GAPN buffer with 40 mM GSH. Concentrations were determined using Bradford assays with BSA standards, and protein was stored in 40% glycerol at -20 °C. GAP

assays were performed as described by Cowan *et al.*²⁵ in GAPN buffer with 15 μM rhodopsin (in urea washed bovine rod outer segment membranes), 1 μM G_{tu}, 50 nM GTP, 1 μM RGS, ± 2 μM PDE γ . Time points were recorded at various times after the addition of GTP by quenching the reaction with 5% TCA. The time course of GTP hydrolysis was fit to the single exponential: %GTP hydrolyzed = (1 - exp[-k_{inact} × time]) × 100%. The Δk_{inact} for each RGS protein was calculated as $\Delta k_{inact} = (k_{inact}(RGS + G_{tu}) - k_{inact}(G_{tu}))$.

Acknowledgments

This work was supported by NIH, NLM, the Welch Foundation, and the Keck Center for Computational Biology. M.A.K. is a Howard Hughes Medical Institute Fellow of the Life Sciences Research Foundation. O.L. gratefully acknowledges the support of the American Heart Association and NHGRI.

Correspondence should be addressed to O.L. *email:* lichtarge@bcm.tmc.edu

Received 6 December, 2000; accepted 22 January, 2001.

1. Cowan, C.W., He, W. & Wensel, T.G. *Prog. Nucl. Acid Res. Mol. Biol.* **65**, 341–359 (2000).
2. Benzing, T. *et al. J. Biol. Chem.* **275**, 28167–28172 (2000).
3. Zheng, B., Chen, D. & Farquhar, M. *Proc. Natl. Acad. Sci. USA* **97**, 4040–4045 (2000).
4. Kovoov, A. *et al. J. Biol. Chem.* **275**, 3397–3402 (2000).
5. Posner, B.A., Gilman, A.G. & Harris, B.A. *J. Biol. Chem.* **274**, 31087–31093 (1999).
6. McEntaffer, R.L., Natochin, M. & Artemyev, N.O. *Biochemistry* **38**, 4931–4937 (1999).
7. Nekrasova, E.R. *et al. Biochemistry* **36**, 7638–7643 (1997).
8. Natochin, M., Granovsky, A.E. & Artemyev, N.O. *J. Biol. Chem.* **272**, 17444–17449 (1997).
9. Popov, S., Krishna, U., Falck, J. & Wilkie, T. *J. Biol. Chem.* **27**, 18962–18968 (2000).
10. Womack, K. *et al. J. Neurosci.* **20**, 2792–2799 (2000).
11. Tu, Y., Popov, S., Slaughter, C. & Ross, E. *J. Biol. Chem.* **274**, 38260–38267 (1999).
12. Chen, C., Seow, K.T., Guo, K., Yaw, L.P. & Lin, S.C. *J. Biol. Chem.* **274**, 19799–197806 (1999).
13. Druey, K.M. *et al. J. Biol. Chem.* **274**, 18836–18842 (1999).
14. Lichtarge, O., Bourne, H.R. & Cohen, F.E. *J. Mol. Biol.* **257**, 342–358 (1996).
15. Sowa, M.E., He, W., Wensel, T.G. & Lichtarge, O. *Proc. Natl. Acad. Sci. USA* **97**, 1483–1488 (2000).
16. He, W., Cowan, C.W. & Wensel, T.G. *Neuron* **20**, 95–102 (1998).
17. Makino, E.R., Handy, J.W., Li, T. & Arshavsky, V.Y. *Proc. Natl. Acad. Sci. USA* **96**, 1947–1952 (1999).
18. Chen, C.K. *et al. Nature* **403**, 557–560 (2000).
19. Arshavsky, V. & Bownds, M.D. *Nature* **357**, 416–417 (1992).
20. Lichtarge, O., Bourne, H.R. & Cohen, F.E. *Proc. Natl. Acad. Sci. USA* **93**, 7507–7511 (1996).
21. Lichtarge, O., Yamamoto, K.R. & Cohen, F.E. *J. Mol. Biol.* **274**, 325–337 (1997).
22. Onrust, R. *et al. Science* **275**, 381–384 (1997).
23. Slep, K.C. *et al. Nature*, **in the press** (2001).
24. Tesmer, J.J., Berman, D.M., Gilman, A.G. & Sprang, S.R. *Cell* **89**, 251–261 (1997).
25. Cowan, C.W., Wensel, T.G. & Arshavsky, V.Y. *Methods Enzymol.* **315**, 524–538 (2000).
26. Nicholls, A., Sharp, K. & Honig, B. *Proteins* **11**, 281–296 (1991).
27. Kraulis, P. *J. Appl. Crystallogr.* **24**, 946–950 (1991).
28. Merritt, E. & Bacon, D. *Methods Enzymol.* **277**, 505–524 (1997).